*Research Article* *ISSN: 2319-507X*
*Amrut Lanje, IJPRET, 2013; Volume 1(8): 54-63* *IJPRET*


**INTERNATIONAL JOURNAL OF PURE AND APPLIED RESEARCH IN ENGINEERING AND TECHNOLOGY**

A PATH FOR HORIZING YOUR INNOVATIVE WORK

# X-RAY PHOTOELECTRON SPECTROSCOPY AND LUMINESCENCE STUDIES OF Fe DOPED ZnO NANOPARTICLES

**AMRUT LANJE[1], SATISH SHARMA[2], RAGHUMANI NINGTHOUJAM[3]**

1. Department of Electronics, Dr. Ambedkar College, Chandrapur - 442 401, India
2. Department of Electronics, R .T. M. Nagpur University, Nagpur - 440 033, India
3. Chemistry Division, Bhabha Atomic Research Center, Mumbai - 400 085, India.

**Accepted Date:**
27/02/2013
**Publish Date:**
01/04/2013

**Keywords**
Nanoparticles,
Zinc oxide,
Photoluminescence,
doping

**Corresponding Author**
**Mr. Amrut Lanje**

## Abstract

Iron (Fe) doped Zinc Oxide (ZnO) nanoparticles are prepared by urea hydrolysis method at relatively low temperature at 130 °C. Unit cell volume increases with $Fe^{2+}$ ions doping in ZnO indicating substitution of $Zn^{2+}$ sites by $Fe^{2+}$ ions. X-ray photoelectron spectroscopy (XPS) was used to study surface chemical state of the Fe doped nanoparticles. XPS study reveals that Fe ions in the sample are mainly in the chemical state of $Fe^{2+}$. The crystallite sizes are in range 52-62 nm. Photoluminescence intensity decreases with increase in $Fe^{2+}$ doping concentration in ZnO. The wavelength corresponding to the band-edge emission decreases from 399 to 392 nm upon doping with $Fe^{2+}$ ions in ZnO. Similarly, the band-edge absorption peak shifts slightly to lower wavelength when ZnO is doped with $Fe^{2+}$ ions. It is established that band gap of ZnO increases slightly on $Fe^{2+}$ ions in ZnO lattice.

## INTRODUCTION

Many researchers (Ningthoujam, 2007, Ningthoujam, 2008, Singh, 2008, Gajbhiye 2008 and Gao, 2008) have Studied on the electronic and optical properties of semiconductor which has potential applications in solar cells, lasers, spintronics and fluorescent tags in biotechnology. The research field of spintronics emerged from experiments on spin-dependent electron transport phenomena in solid-state devices. Presently, several researchers (Dietl, *et al.* 2000 and Alaria, *et al.* 2006) are investigating the diluted magnetic semiconductors (DMS). DMS are "conventional" semiconductors doped with transition metal or rare earth ions which are diluted within host of matrix and ferromagnetically aligned via an indirect magnetic coupling (Wolf, *et al.* 2001).

Various preparation techniques have been used for the preparation of ZnO based DMS material. Polyakov, *et al.* (2004) has reported the room temperature ferromagnetism by implanting Fe ions in ZnO crystal grown by vapor phase. Potzger, *et al.* (2006) also observed room temperature ferromagnetism by implanting Fe ions in hydrothermal ZnO single crystal. Mandal, *et al.* (2006) reported the preparation of Fe-doped ZnO nanoparticles. Solid state reaction, sol-gel method, hydrothermal and mechanical alloying methods have been employed by Saha and Ali (1997) for the preparation of Fe-doped ZnO.

In the present work, we have synthesized the Fe doped ZnO nanoparticles using urea hydrolysis in ethylene glycol medium at relatively low temperature of 130 °C. Ethylene glycol is the most suitable capping agent/surfactant since it has a lower molecular formula and helps to avoid the reducing luminescence intensity compared to other surfactant. X-ray photoelectron spectroscopy (XPS) and luminescence properties of synthesized Fe doped ZnO particles samples suggests the substitution of $Fe^{2+}$ in $Zn^{2+}$ site of ZnO in small amount and most $Fe^{3+}$ ions form $\alpha$-$Fe_2O_3$ as a secondary phase.

## MATERIALS AND METHODS

### Chemicals

All the chemicals were of analytical grade and used as received without further purification. Deionized water was used throughout the experiment. Zinc acetate,

iron (II) sulphate heptahydarate and ethylene glycol were supplied by Merck. Urea was procured from the Qualigens Fine Chemicals (Mumbai, India).

**Synthesis**

In a typical preparation of Fe doped ZnO with Zn/Fe ratio of 0.98/0.02, 1 g of zinc acetate and 0.025 g of iron (II) sulphate heptahydrate were dissolved in 100 ml ethylene glycol in a round bottom flask. After complete dissolution, 5 g of urea and 50 ml of distilled water were added to above solution and stirred using the magnetic stirrer for 15 min. The solution was heated at 130 °C for 2 h. The white precipitate appears. After cooling at room temperature, the obtained precipitate was centrifuged. To remove the excess ethylene glycol, the precipitate was again centrifuged and further washed by adding methanol and acetone. The obtained precipitate was then dried at 100 °C for 5 h. similar process is repeated for obtaining others Fe doped ZnO with Zn/Fe ratio of 0.95/0.05, 0.90/0.1. Figure 1 displays the schematic diagram of preparation of Fe doped ZnO.

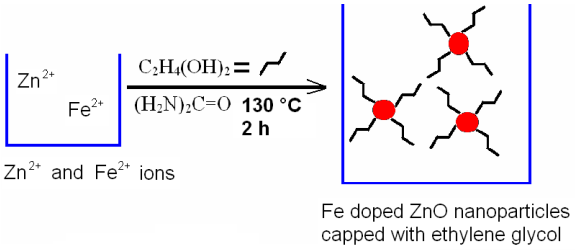


**Figure 1 Schematic diagram of the preparation of Fe-doped ZnO nanoparticles**

**Characterization**

The powder X-ray diffraction (XRD) was performed using Philips Holland, XRD system PW 1710 with nickel filtered Cu $K_\alpha$ ($\lambda$ = 1.54056 Å) radiation. The average crystallite size ($t$) was calculated from the line broadening using the Scherrer's relation: $t = 0.9\lambda/B\cos\vartheta$ where $\lambda$ is the wavelength of X-ray and $B$ is the half maximum line width. The FT-IR spectra were recorded using Bomen Hartmann & Braun MB Series Infrared spectrometer. In acquire the knowledge of the chemical state of constituent elements, XPS spectra were measured with a CLAM-2 analyzer (VG make) spectrometer using the $MgK_\alpha$ source (1253.6 eV) operated at 15 kV, 20 mA. The system pressure in the range of $10^{-9}$ Pa and the area of 7 ×4 $mm^2$ for the sample surface analysis were used for the measurements. Survey and higher resolution (narrow scan)

spectra were measured with pass energies set at 192 and 48 eV, respectively. Photoluminescence (PL) measurements were performed by using F-4500 FL spectrophotometer with 150 W Xenon lamp at room temperature. Powder samples were spread over a glass slide and mounted inside the sample holder for PL measurements.

## RESULTS AND DISCUSSION

### XRD Study

Figure 2 shows the X-ray diffraction patterns of pure ZnO and Fe doped ZnO with Zn/Fe ratio of 0.98/0.02, 0.95/0.05, 0.90/0.1. These samples demonstrate the hexagonal structure of ZnO. The estimated lattice parameters of pure ZnO (x = 0) are $a$ = 3.255(1), $c$ = 5.206(1) Å and its unit cell volume is $V$ = 47.7 Å$^3$. These values are in good agreement with the reported values (JCPDS file No. 05-664). Secondary phase of $\alpha$-$Fe_2O_3$ (peak at 33.19° in 2theta, JCPDS file no. 33-0664) is also observed. Slight increase in unit cell volume (2%) of ZnO for the Fe doped ZnO indicates that a few $Fe^{2+}$ ions occupy $Zn^{2+}$ sites of ZnO lattice. Based on Scherer's relation, the average crystallite sizes are found to be in the range 50 to 60 nm, corroborating the formation of nano crystals.

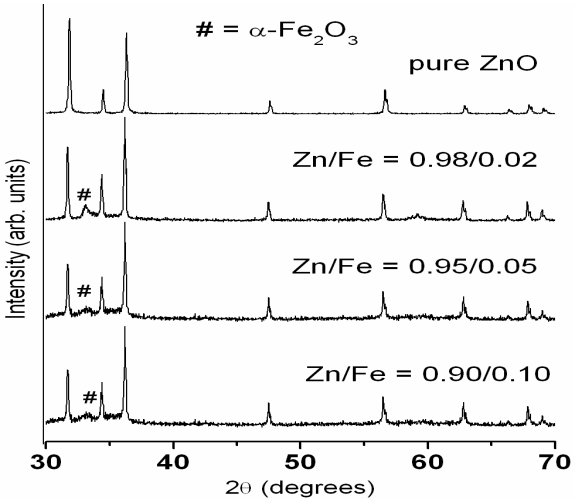


**Figure 2 X-ray diffraction patterns of pure ZnO and Fe doped ZnO with Zn/Fe ratio of 0.98/0.02, 0.95/0.05, 0.90/0.10**

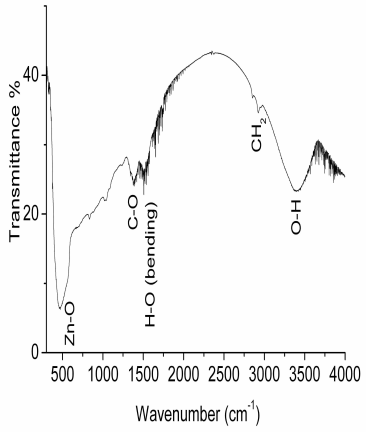


**Figure 3 IR spectrums of as-prepared ZnO nanoparticles.**

### IR Study

Figure 3 shows the IR spectrum of as-synthesized ZnO nanoparticles. The O-H, C-H, C-O functional groups in addition to Zn-O

bond are attributed to the functional groups/bonds present in ethylene glycol molecules, which act as capping.

However, the stretching frequency of free O-H is at 3650 $cm^{-1}$ (Kemp, 1975). In this study, the red shifted broad band at 3402 $cm^{-1}$ is a signature of the presence of hydrogen bond in ethylene glycol molecules. The wagging vibration at 1287 $cm^{-1}$, twisting vibration at 1027 $cm^{-1}$ and rocking vibration at 831 $cm^{-1}$ due to presence of $CH_2$ are observed which hinder agglomeration among particles. The O-H bond recorded at 3000-3400 $cm^{-1}$ can interact with the methanol or ethanol (organic solvent) through the inter-H-bonding (Karve, *et al.* 2000, An, *et al.*1998, Lin, *et al.*1996, Fuentes, *et al.* 2006 and Yang, *et al.* 2006).

**XPS Study**

Figure 4 shows the typical survey XPS spectrum for Fe doped ZnO with Zn/Fe ratio of 0.90/0.10. Zinc, oxygen and iron peaks

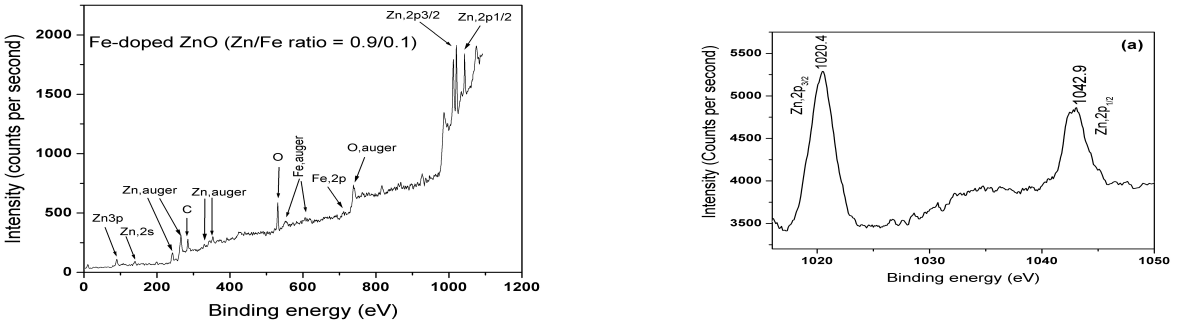


**Figure 4 The survey XPS spectrum of Fe-doped ZnO with Zn/Fe ratio of 0.90/0.10**


**Figure 5 XPS spectra of (a) Zn 2p, (b) Fe 2p and (c) O 1s in Fe-doped ZnO with Zn/Fe ratio of 0.90/0.10**

are observed. In addition to these, carbon peak is also found for standard calibration.

Figure 5 (a) shows that the Zn $2p_{3/2}$ is situated at 1020.4 eV and Zn $2p_{1/2}$ is at 1042.9 eV indicating Zn ions in the sample are mainly in the chemical state of $Zn^{2+}$ (Chen, et al. 2006). Figure 5 (b) shows the XPS spectrum of Fe 2p. The peaks at 709.63 and 723.3 eV correspond to Fe $2p_{3/2}$ and Fe $2p_{1/2}$, respectively indicating that some Fe ions are in $Fe^{2+}$ state. The energy difference spectrum at 530.8 eV is attributed to O lattice in wurtzite structure of hexagonal Zn ion array (Cebulla, *et al.* 1998, and Rao & Vinni 1993).

**Luminescence Study**

The room temperature photoluminescence spectra of pure ZnO and Fe doped ZnO with Zn/Fe ratio of 0.98/0.02, 0.95/0.05, 0.90/0.10 after excitation at 320 nm are shown in Figure 6. In pure ZnO, the prominent peaks at 399 and 469 nm due to band-edge-emission and artifact are observed (Ningthoujam, *et al.* 2007, and Singh, *et al.* 2008). On increasing the Fe concentration in ZnO, the peak intensity decreases and the band edge emission between Fe $2p_{3/2}$ and Fe $2p_{1/2}$ is 13.6 eV. Earlier, similar result has been reported by Zhao, et al. (2007) for $Fe^{2+}$ state. Also, $Fe^{3+}$ state could be observed at Fe $2p_{3/2}$ (711.5 eV), confirming the formation of $\alpha$-$Fe_2O_3$ as secondary phase. The satellite appeared at 7-8 eV above the parent peak is due to multiple interactions of oxides and hydroxide (Sudakar, *et al.* 2004). Figure 5(c) shows the XPS spectrum of O 1s. The low binding energy component of the O 1s shifts from 399 to 392 ± 2 nm. This is expected as the presence of $Fe^{2+}$/$Fe^{3+}$ impurity reduces the luminescence intensity. At a close look into spectrum, a broad hump around 545 nm can be attributed to singly ionized oxygen vacancy in ZnO materials.

Figure 7 shows the excitation spectra of pure ZnO and Fe doped ZnO with Zn/Fe ratio of 0.98/0.02, 0.95/0.05, 0.90/0.10 monitored at 520 nm. The intensity decreases with the increase of Fe concentrations in ZnO. The observed trend is similar to the emission spectra. Inset of this figure shows the expansion of excitation spectra. The band edge absorption around 355-375 nm is observed,

which is similar to reported value of pure ZnO (Yatsui, *et al.* 2002). However, the wavelength corresponding to the band edge absorption decreases slightly with the $Fe^{2+}$ doping. This is reflected in the emission spectra where wavelength corresponding to the band-edge emission decreases from 399 to 392 nm. These results establish the slight increase of band gap with the Fe doping in ZnO.

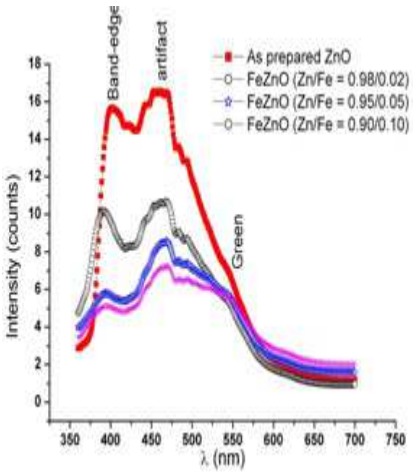


**Figure 6 PL emission spectra of pure ZnO and Fe doped ZnO after 330 nm excitation.**

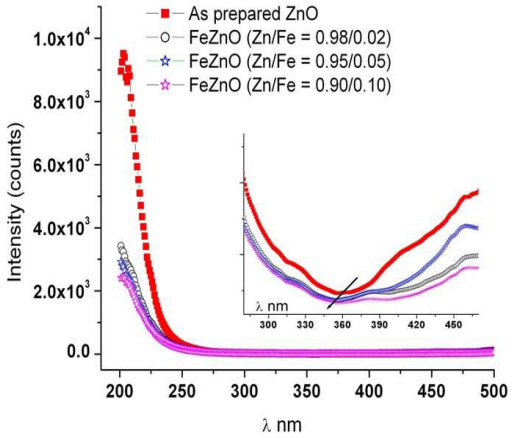


**Figure 7 Excitation spectra of pure ZnO and Fe doped ZnO at 520 nm.**

## CONCLUSIONS

Pure ZnO and Fe doped ZnO with Zn/Fe ratio of 0.98/0.02, 0.95/0.05, 0.90/0.10 nanoparticles were synthesized at relatively low temperature (130°C). Secondary phase of $\alpha$-$Fe_2O_3$ was reported. XPS study revealed that Zn ions in the sample are mainly in the chemical state of $Zn^{2+}$ while $Fe^{n+}$ ions are in $Fe^{2+}$ and $Fe^{3+}$ states for Fe doped ZnO. PL Luminescence intensity decreases with the increase of Fe concentrations in ZnO indicating that the Fe impurity produces quenching centers in luminescence. Enhanced band gap for Fe doped ZnO as compared to that of pure ZnO is noted.

## ACKNOWLEDGMENTS

Authors are thankful to Dr. D. Das, Chemistry division for encouragement during the work and Mr. Jagannath, TPPED, Bhabha Atomic Research Center, Mumbai for providing XPS data. Authors are also grateful to Dr. Ajay Gupta and his colleagues, UGC-DAE Consortium for

Scientific Research Center, Indore for providing XRD data.

**REFERENCES**

1. Alaria J, Bouloudenine M, Schmerber G, Colis S, Dinia A, Turek P and Bernard M, Pure paramagnetic behavior in Mn-doped ZnO semiconductors, J. Appl. Phys., 2006; 99: 08M118.

2. An D, Yue Z and Chen RT, Dual-functional polymeric waveguide with optical amplification and electro-optic modulation, Appl. Phys. Lett., 1998; 72: 2806.

3. Cebulla R, Wendt R and Ellmer K, Al-doped zinc oxide films deposited by simultaneous rf and dc excitation of a magnetron plasma: Relationships between plasma parametersand structural and electrical film properties, J. Appl. Phys., 1998; 83, 1087.

4. 4. Chen JT, Wang J, Zhang F, Zhang GA, Wu ZG, and Yan PX, The effect of La doping concentration on the properties of zinc oxide films prepared by the sol–gel method, J. Cryst. Growth, 2008; 310: 2627.

5. Dietl T, Ohno H, Matsukura F, Cibert J and Ferrand D, Zener Model Description of Ferromagnetism in Zinc-Blende Magnetic Semiconductors, Science, 2000; 287: 1019

6. Fuentes M, Mateo C, Rodriguez A, Casqueiro M, Tercero JC, Riese HH, Fernandez-Lafuente R and Guisan JM, Detecting minimal traces of DNA using DNA covalently attached to superparamagnetic nanoparticles and direct PCR-ELISA, Biosens. and Bioelectron., 2006; 21: 1574.

7. Gajbhiye NS, Ningthoujam RS, Ahmed A, Panda DK, Umre SS and Sharma SJ, Re-dispersible Li+ and $Eu^{3+}$ co-doped CdS nanoparticles: Luminescence Studies, Pramana, 2008; 70: 313.

8. Gao J, Zhang W, Huang P, Zhang B and Xu B, Intracellular Spatial Control of

9. Fluorescent Magnetic Nanoparticles, J. Am. Chem. Soc., 2008; 130: 3710.

10. Karve G, Bihari B and Chen RT, Demonstration of optical gain at 1.06 µm in a neodymium-doped polyimide waveguide, Appl. Phys. Lett., 2000; 77: 1253.

11. Kemp W, Organic Spectroscopy, Macmillan, Hampshire, 1975.

12. Lin S, Feuerstein J and Mickelson AR, Study neodymium-chelate-doped optical

polymer wave guides, J. Appl. Phys., 1996; 79: 2868.

13. Mandal SK, Nath TK, Das A and Kremer RK, Magnetic glassy phase in $Zn_{0.85}Fe_{0.15}O$ diluted magnetic semiconducting nanoparticles, Appl. Phys. Lett., 2006; 89: 162502.

14. Nakamoto K, Infrared and Raman Spectra of Inorganic and Coordination Compounds, Wiley, New York, 1986.

15. Ningthoujam RS, Sudarsan V, Tyagi AK, Vinu A, Srinivasu P, Ariga K and Kulshreshtha SK, Luminescence, lifetime, and quantum yield studies of redispersible $Eu^{3+}$-doped $GdPO_4$ crystalline nanoneedles: Core-shell and concentration effects, J. Nanosci. Nanotech., 2008; 8: 1489.

16. Ningthoujam RS, Sudarsan V, Godbole SV, Kienle L, Kulshreshtha SK and Tyagi AK, $SnO_2$:$Eu^{3+}$ nanoparticles dispersed in $TiO_2$ matrix: Improved energy transfer between semiconductor host and $Eu^{3+}$ ions for the low temperature synthesized samples, Appl. Phys. Lett., 2007; 90: 173113.

17. Ningthoujam RS, Sudarsan V and Kulshreshtha SK, $SnO_2$:Eu nanoparticles dispersed in silica: A low-temperature synthesis and photoluminescence study, J. Lumin., 2007; 127: 747.

18. Polyakov AY, Govorkov AV, Smirnov NB, Pashkova NV, Pearton SJ, Ip K, Frazier RM, Abernathy CR, Norton DP, Zavada JM and Wilson RG, Optical and magnetic properties of ZnO bulk crystals implanted with Cr and Fe, Mater. Sci. Semicond. Process, 2004; 7: 77.

19. Potzger K, Zhou SQ, Reuther H, Mücklich A, Eichhorn F, Schell N, Skorupa W, Helm M, Fassbender J, Herrmannsdörfer T and Papageorgiou TP, Fe Implanted ferromagnetic ZnO, Appl. Phys. Lett., 2006; 88: 052508.

20. Rao LK and Vinni V, Novel mechanism for high speed growth of transparent and conducting tin oxide thin films by spray pyrolysis, Appl. Phys. Lett., 1993; 63: 608.

21. Saha S and Ali N, Magnetic properties of the $Pr_{1-x}La_xMnGe$ system, J. Appl. Phys., 1997; 81: 4212.

22. Singh LR, Ningthoujam RS, Sudarsan V, Srivastava I, Singh SD, Dey GK and Kulshreshtha SK, Luminescence study on $Eu^{3+}$ doped $Y_2O_3$ nanoparticles: particle size, concentration and core–shell formation effects, Nanotechnology, 2008; 19: 055201.

23. Singh LR, Ningthoujam RS, Sudarsan V, Singh SD and Kulshreshtha SK, Probing of surface $Eu^{3+}$ ions present in ZnO:Eu nanoparticles by covering ZnO:Eu core with $Y_2O_3$ shell: Luminescence study, J. Lumin., 2008; 128: 1544.

24. Sudakar C and Kutty TRN, Structural and magnetic characteristics of cobalt ferrite-coated nano-fibrous γ-$Fe_2O_3$ J. Magn. Magn. Mater., 2004; 279: 363.

25. Wolf SA, Awschalom DD, Buhrman RA, Daughton JM, Molnár S, Roukes ML, Chtchelkanova AY and Treger DM, Spintronics: A Spin-Based Electronics Vision for the Future, Science, 2001; 294: 1488.

26. Yang L, Shen Q, Zhou J and Jiang K, Biomimetic synthesis of CdS nanocrystals in aqueous solution of pepsin, Mater. Chem. Phys., 2006; 98: 125.

27. Yatsui T, Kawazoe T, Schmizu T, Yamamoto Y, Ueda M, Kourogi M, Ohtsu M, and Lee GH, Observation of size-dependent features in the photoluminescence of zinc oxide nanocrystallites by near-field ultraviolet spectroscopy, Appl. Phys. Lett., 2002; 80: 1444.

28. Zhao D, Wu X, Guan H and Han E, Study on supercritical hydrothermal synthesis of CoFe2O4 nanoparticles, J. Supercrit. Fluids, 2007; 42: 226